

Article

Real-Time Identification and Positioning of Sewer Blockage Based on Liquid Level Analysis in Rural Area

Ning Li ¹, Xiaodong Wang ^{1,*} , Zhichao Li ¹, Fangchao Zhao ¹, Abhilash Nair ² , Junxiao Zhang ³ and Changqing Liu ¹

¹ School of Environmental and Municipal Engineering, Qingdao University of Technology, Jialingjiang Dong 777, Huangdao, Qingdao 266520, China

² DOSCON AS, P.B. 53 Vollebekk, 0516 Oslo, Norway

³ Rongcheng Water Group, Guanhai Dong 6, Rongcheng 264300, China

* Correspondence: wangxiaodong@qut.edu.cn

Abstract: Sewer blockages delay sewage discharge or cause it to overflow, which pollutes the environment and is a public health hazard. This necessitates the quick and accurate identification and positioning of sewer blockages. Following a sewer blockage, the sewage is intercepted and the liquid level at the upstream and downstream of the blocking point changes. This study established a method for identifying sewer blockages by analyzing the range and rate of the liquid level change at the upstream and downstream of the blocking point. Through pilot-scale and full-scale experiments, this study summarized the threshold values of the liquid level change rate and the liquid level fluctuation range of the drainage pipeline in normal operation, as well as the threshold values of the liquid level change rate and the liquid level fluctuation range of the upstream and downstream of the sewer blocking point. Moreover, the sewer blockage identification matrix was completed. Sewer blockage in rural areas can be identified and positioned using mathematical tools such as the data-driven model. This research method allows for real-time monitoring and timely warning of the sewer status, thereby reducing the labor and material consumption and unnecessary earthwork excavation to ensure the stable operation of the drainage pipeline.

Keywords: identification and positioning; sewer blockage; liquid level analysis; data-driven models; rural area



Citation: Li, N.; Wang, X.; Li, Z.; Zhao, F.; Nair, A.; Zhang, J.; Liu, C. Real-Time Identification and Positioning of Sewer Blockage Based on Liquid Level Analysis in Rural Area. *Processes* **2023**, *11*, 161. <https://doi.org/10.3390/pr11010161>

Academic Editor: Vicenç Puig

Received: 15 November 2022

Revised: 24 December 2022

Accepted: 29 December 2022

Published: 4 January 2023



Copyright: © 2023 by the authors. Licensee MDPI, Basel, Switzerland. This article is an open access article distributed under the terms and conditions of the Creative Commons Attribution (CC BY) license (<https://creativecommons.org/licenses/by/4.0/>).

1. Introduction

The stable operation of sewers, which serve as the main tool for transporting domestic sewage, is very important, and both developing and developed countries pay considerable attention to the sewer network. In 2016, the lengths of China's urban sewer and drainage pipes increased by 5.7% and 2.4% from 577,000 km and 172,000 km in the previous year, respectively [1]. In addition, drainage pipes in cities and rural areas will be increasingly optimized owing to societal development [2–4]. Sewer operation exhibits challenges such as blocking, siltation and leakage, and hidden dangers such as sewage overflow, poor drainage, and soil and groundwater pollution. Owing to the different social functions of cities and rural areas, the characteristics of sewage discharge vary. Sewage from various urban areas is collected by sewer and transported to the wastewater treatment plant for collective treatment. However, rural areas report low sewage collection rate and water volume. In addition, sediment, domestic garbage, crop straw, and other substances are easy to deposit owing to the lack of water flow power in the sewer, thereby clogging of the sewer [5]. The small diameter of the sewers (DN100–DN300), and inferior operation and maintenance management in rural areas limit the stable operation of sewers. Studies show that sewer blockage is related to pipe diameter, slope, and pipeline aging degree [6]. Efficient and accurate identification and positioning of sewer blockage can reduce the need for earthwork excavation and are conducive to environmental protection and waterlogging mitigation.

Most sewer detection technologies use video, sonar, radar, and ultrasonic sensors among others to detect the internal conditions of pipelines via in-pipe robots [7–10]. Each of these sewer detection methods has unique advantages and application conditions. Closed circuit television video (CCTV) analysis and laser detection are used to determine the pipeline status by moving the traction tool fitted with CCTV or a laser transmitter to obtain the video picture data inside the pipeline or the three-dimensional model of the pipeline based on the laser processing software. Real-time monitoring of the sewer using this detection method is difficult and has requirements on the diameter of the sewer [11]. Following the development of electric control and computer technologies, in-pipe robots have advanced over time. In-pipe robots can perform different functions for sewer status detection [9,12] and pipeline repair [8] among other operations; however, the complex situation in the drainage pipeline continues to be a challenge for pipeline robots [13,14]. Following the development of research, in-pipe robots have stronger adaptability and trafficability to drainage pipelines. The robot acquires the internal information of the sewer by carrying different sensors such as vision, laser, and sonar and completes the pipeline state evaluation and abnormality diagnosis through machine learning methods. At present, the in-pipe robots can replace manual repair of pipeline leakage, root intrusion, pipeline deformation, and pipeline dredging. The acoustic detection method has outstanding advantages; for example, the complex pipeline information can be provided through the acoustic signal, and the detection method is simple and low-cost. However, it is limited by the fault extraction method of the acoustic signal and low discrimination between fault features [15–17]. Various machine learning methods play an important role in sewer status detection, including the use of machine learning methods such as qualitative trend analysis [18,19], random forest [20], and support vector machine [21], which allow for data-driven drainage pipeline status monitoring technology [22]. However, the limitations of each monitoring technology limit the effect of on-site use. This urgently necessitates real-time monitoring technology that is not limited by the diameter of the sewer and internal conditions to monitor the sewer in real time and provide warnings for fault occurrence.

After sewer blockage, the sewage interception causes abnormal fluctuation of the upstream and downstream liquid levels at the blocking point. Therefore, monitoring the liquid level at the upstream and downstream of the blocking point to obtain the change rule of the upstream and downstream liquid levels at the blocking point for blocking identification is feasible. With Internet of Things (IOT), real-time massive monitoring for detection has become possible. This type of study has become relevant with IoT sensors, as massive monitoring is a prerequisite. Presently, numerous products with ultrasonic sensors are widely used in various fields, such as liquid level monitoring, which can be combined to conduct real-time monitoring of urban rain flood conditions. Evidently, liquid level monitoring plays an important role in urban drainage and rain flood management [23]. The drainage system in rural areas has monitoring difficulties such as low flow and pipe diameter. The accuracy of the liquid level sensor is 1 mm [24]; therefore, multiple liquid level sensors are required to form a liquid level monitoring network for the identification and positioning of the blockage.

In this study, through pilot-scale and full-scale experiments, the change rule of liquid level upstream and downstream of the sewer blockage is studied, and then the identification and positioning matrix of sewer blockage is determined. This paper is divided into four sections. The first section introduces the background of the identification and positioning of sewer blockage and the feasibility of this method. The second section describes the experimental design, pilot-scale and full-scale experiments, and data pre-processing of sewer blockage identification and positioning. The third part introduces the experiment conclusions of the pilot-scale and full-scale experiments of the sewer and realization process of the blockage identification. The fourth section summarizes the study and prospects of the proposed method.

2. Materials and Methods

2.1. Experimental Design

The experimental design of this research method is shown in Figure 1. Sewer blockage identification and positioning were performed as follows. The installation positions of the liquid level sensors were determined according to the different blockage positions. The liquid level sensors were installed upstream and downstream of and in close proximity to the blockage point, and the relevant pilot-scale and full-scale experiments were performed. The experimental data were uploaded to the cloud in real time. The experimental data were obtained, and the moving average method was used to pre-process the data. Afterwards, the data and derivative were analyzed to obtain the sewer blockage identification matrix for on-site application.

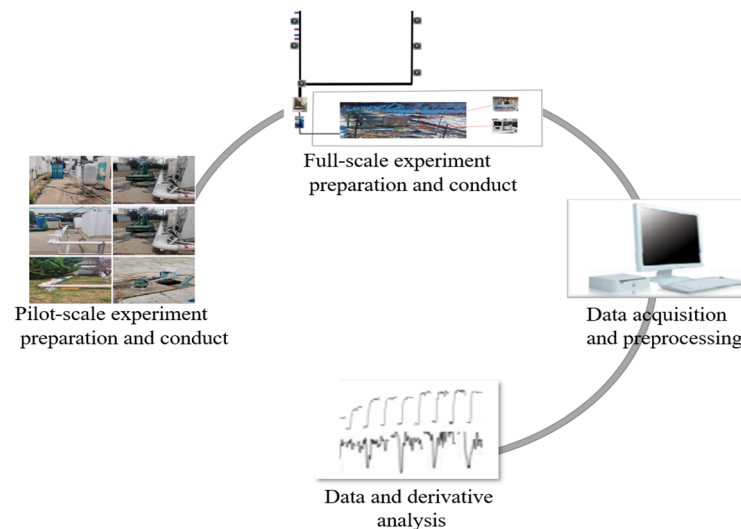


Figure 1. Experimental design for the identification and positioning of sewer blockage.

2.2. Pilot-Scale Experimental Setup for Sewer Blockage Identification

The pilot-scale experimental system of this study was built in a wastewater treatment plant in Qingdao. It was designed and constructed according to the design specifications. As shown in Figure 2a, the total length of the sewer was 81.6 m, and the pipe diameters of DN100, DN150, DN200, and DN300 increased from upstream to downstream, and the pipe is made of polyvinyl chloride. The corresponding diameters, slopes, lengths, and the spacing between manholes of each pipe section are shown in Table 1. In the pilot-scale experiment, the water inlet of the wastewater treatment plant was used. During the test, the pump transported water into the storage tank. The flow in the sewer was controlled by adjusting the opening and closing degree of the valve on the outlet side of the water tank; flow rates range from $0.5 \text{ m}^3/\text{h}$ to $5 \text{ m}^3/\text{h}$, with each experiment increasing by $0.5 \text{ m}^3/\text{h}$. Only one experiment was performed per set, and there were no replicates. A total of seven manholes were organized at each node of the sewer at the reducers and bends, and the liquid level of each manhole of the drainage pipeline was monitored in real time using three movable liquid level sensors. The dash lines between the level sensor PL and the manhole PW indicate the manhole that the level sensor PL can be installed. During the experiment, a mixture of toilet paper, leaves, and plastic bags with dry weights of 0.2 kg, 0.15 kg, and 0.1 kg, respectively, were used as the blockage of the drainage pipe. In normal circumstances, sewers only contain household waste such as toilet paper, but through on-site investigation in many villages and towns in Shandong Province of China, it was found that sewers contain leaves, plastic bags, bottles, and other household waste. Therefore, a mixture of plastic bags, toilet paper and leaves was used as a blockage in this experiment. Each set of experiments was performed at a fixed flow rate, and then three different levels of blockage were generated at the PW2 and PW5 manholes of the sewer. Level sensors were installed upstream and downstream of the blockage point. The sampling time of the

level sensor was 15 s, and the duration of each group of experiments was 13 min. Before the start of the experiment, the flow rate was adjusted by adjusting the opening and closing of the outlet valve, and the flow rate was adjusted from 0.5 m³/h to 5 m³/h. The flow range was selected according to the daily water consumption of 40 L per inhabitant, and the population range was 130–1300 people. Figure 2b shows the specific experimental process.

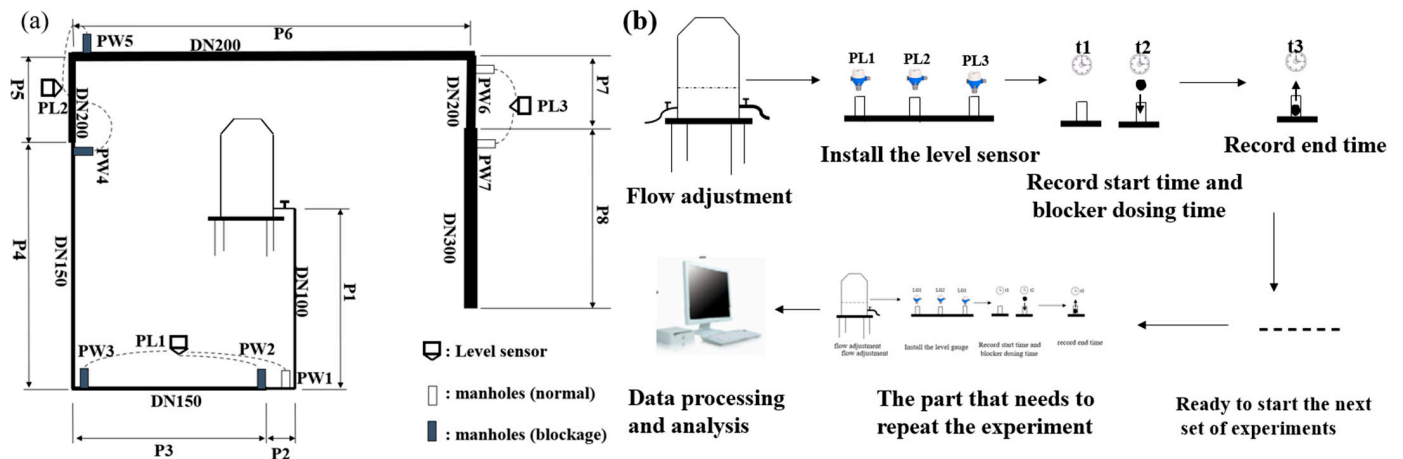


Figure 2. Pilot-scale experimental system for sewer blockage identification. (a) Pilot-scale experimental device of sewer blockage identification. (b) Experimental process of sewer blockage identification.

Table 1. Parameters of the sewer and spacings between manholes.

Serial of Pipe Section	Pipe Diameter (mm)	Install Slope (‰)	Length of Pipe Section (m)	Serial of Manholes	Distance (m)
P1	100	12	14.3	—	Starting end to PW1: 14.65
P2	100	12	1.2	PW1	PW1—PW2: 1
P3	150	7	9	PW2, PW3	PW2—PW3: 8.7 PW3—PW4: 20.85
P4	150	7	20.5	PW4	PW4—PW5: 4
P5	200	5	3.6	—	—
P6	200	5	27	PW5	PW5—PW6: 26.85
P7	200	5	1	PW6	PW6—PW7: 0.85
P8	300	3	5	PW7	PW7 to the pipe end: 4.7

2.3. Full-Scale Experimental Setup for Sewer Blockage Identification

Based on the pilot-scale experiment of sewer blockage identification, the full-scale experimental of sewer blockage identification was carried out in a certain area of Weihai City. According to the survey, there are 220 households in the natural village, and the main source of sewage is kitchen and toilet flushing water. The domestic sewage of each household is collected by the sewer and transmitted to the sewage treatment station for collective treatment. The design scale of the sewage treatment station is 100 m³/d. The annual maximum daily sewage volume in this area is 94.50 m³/d, and the annual average daily sewage volume is 51.86 m³/d. To influence the use function of the sewer in this area, this study conducted full-scale experiments based on the high and low peak consumption periods through investigation, as well as the residents' water use habits. The distribution of high and low peak water consumption periods and the calculation results of the flow in the sewer are shown in Table 2.

Table 2. Peak time period and flow rate of water use in rural areas.

Water Consumption	Time Period	Flow Rate (m ³ /h)
Peak water consumption period	6:30~8:00, 11:00~13:00, 17:30~19:00	3.04
Low water consumption period	The rest of the time	0.87
Hourly average		1.35

In the full-scale experiment, a total of six liquid level sensors were installed at the wellhead of the manholes to monitor the liquid level of the sewer. The arrangement positions of the liquid level sensors are shown in Figure 3. In the figure, FW1, FW2, FW3, and FW4 are the four points that are selected for sewer blockage during the experiment, and FL1, FL2, and FL3 are the three sewer liquid level monitoring points. The right sewer could not be tested because it was blocked during operation and was therefore disregarded in this study. The sewers on the left and right sides collected the domestic sewage of the village, and the sewage flowed through the grid and was transported to the sewage treatment station through the lift pump for collective treatment. The specific experimental process was as follows. During the low water consumption period, a wooden stick with a large number of strips of cloth wrapped around one end is prepared and placed in the manhole to simulate the blockage of the sewer; the FW1 sewer pipe section was blocked, and the start time, t_1 , was recorded. After 10 min, the blockage was removed and the end time t_2 was recorded. Then, the sewer blockage identification experiment of FW2, FW3, and FW4 was performed in the same way. The experimental steps above were repeated during the peak water consumption period.

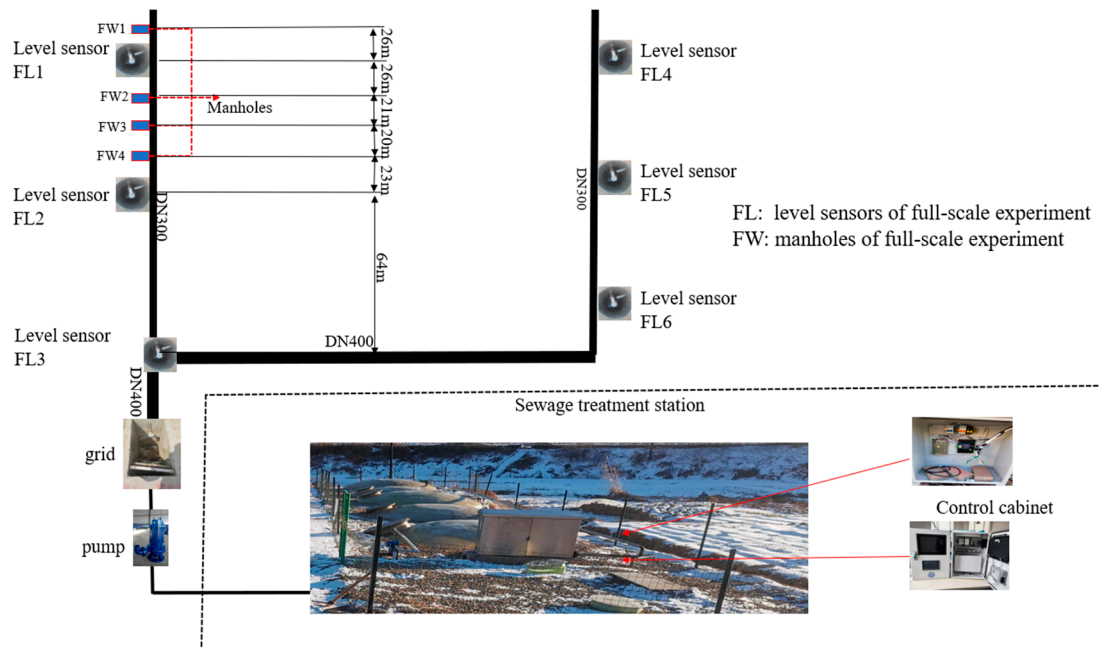


Figure 3. Full-scale experimental system diagram for sewer blockage identification.

2.4. Data Pre-Processing

To reduce the influence of the random error of the level sensor, the moving average method was often used for level data analysis [25]. In this study, the moving average weight of the adjacent time at the same point was 0.5, that is; the measured liquid level at time t_i was H_i ; then the liquid level after the moving average was calculated as Equation (1).

$$\hat{H}_i = 0.5H_{i-1} + 0.5 H_i. \tag{1}$$

Through the analysis of liquid level curve, the liquid level change law before and after drainage pipeline blockage is found, and then the threshold of the liquid level change rate and liquid level change range for blockage identification is found through differential value calculation. Based on this, a double threshold method is obtained to complete the blockage identification of sewers. According to the program diagram shown in Figure 4, the sewer blockage identification program was executed to identify the fault of the drainage pipe blockage. Figure 4a,b represents the lower and upper limits of the threshold value of liquid level change rate after blockage in the sewer, respectively. A and B represent the lower and upper limits of the threshold value of liquid level change range in the sewer, respectively, where a represents the lower threshold of the liquid level change rate under a certain flow rate, which is a positive value. A is the lower threshold of the liquid level change range, which indicates the increase in the value when the liquid level rises, when it tends to be stable, compared with the value before the rise. If the level change rate is greater than a and the level change range is greater than A at the same time, it can be determined that there is a blockage downstream of the level gauge; otherwise it is judged to be normal, where b represents the upper threshold of the liquid level change rate under a certain flow rate, which is negative. B is the upper threshold of the liquid level change range, which indicates the difference between the liquid level after the drop and the liquid level before the drop when the liquid level drops. If the level change rate is less than b and the level change range is less than B at the same time, it can be determined that there is a blockage upstream of the level gauge; otherwise it is judged to be normal. These specific values were derived from the conclusions of the pilot-scale and full-scale experiments.

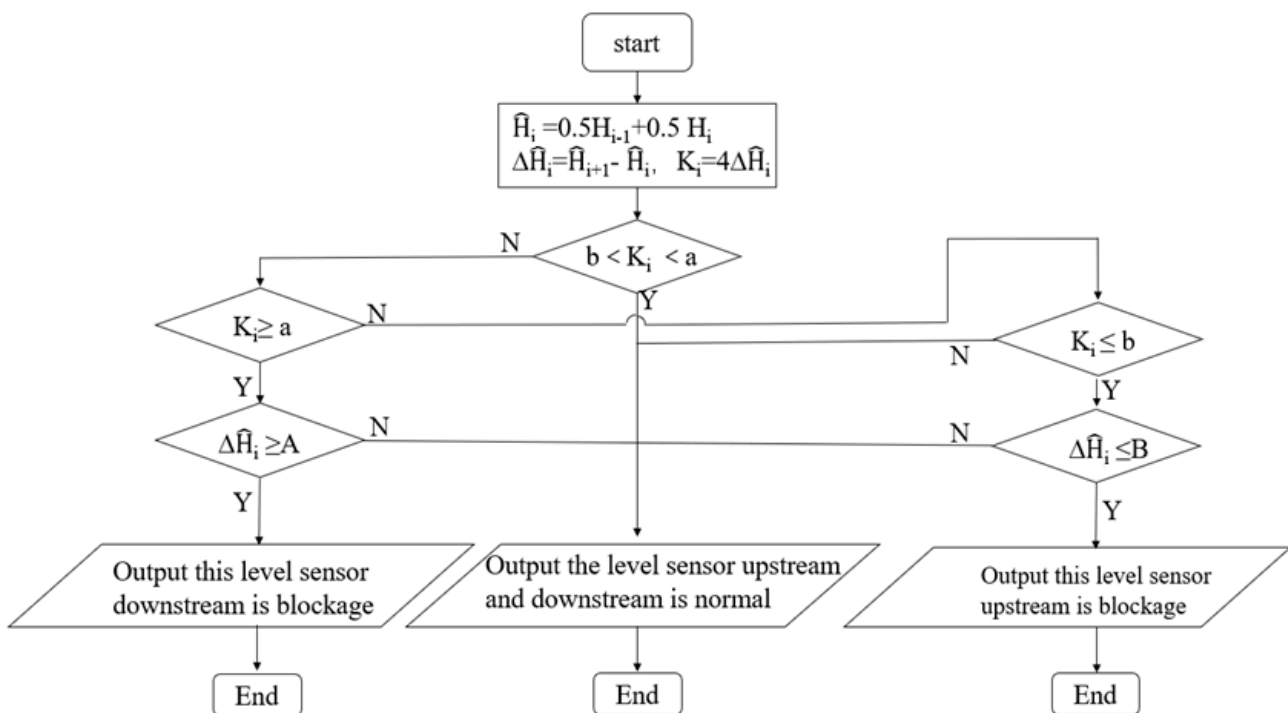


Figure 4. Diagram of the sewer blocking identification procedure.

3. Results and Discussion

3.1. Pilot-Scale Experiment Analysis of Sewer Blockage Identification

In the pilot-scale experiment, after the blockage occurred at PW2 of the DN150 drainage pipe, the liquid level changes at the upstream and downstream of the blockage point in the pipe are shown in Figure 5. After blockage occurs at PW5 of the DN200 drainage pipe, the liquid level changes at the upstream and downstream of the blockage point in the pipe are shown in Figure 6. Figures 5a and 6b show that the sewer is blocked during operation, resulting in poor drainage. Within a minute after the blocking, abnormal

rise in liquid levels can be monitored within 4 m upstream of the blocking point. Within 4 min, the liquid level rises to the peak level, which is 300% to 700% higher than the liquid level before the blockage. Furthermore, the increase in liquid level before the blocking point is positively related to the blocking degree (i.e., the quality of the blocking object) and the flow rate. Figure 6a shows a blockage at PW5 of the sewer with a pipe diameter of DN200, and no obvious liquid level rise is detected at 24.85 m upstream, which indicates that the upstream liquid level rises after the blockage occurs. However, when the liquid level monitoring point is in far proximity from the blockage point, the liquid level rise cannot be monitored for a short time, which gives the relevant operation and maintenance personnel time to accurately position the blockage of the sewer and remove the blocking substances to avoid sewage overflow. Figure 5b,c and Figure 6c show that after the sewer was blocked, the liquid level drop that differed from the normal liquid level fluctuation occurred severally at the downstream of the blocking point, and the change in liquid level drop was continually transmitted downstream. Figure 5c shows that after the sewer with DN150 pipe diameter was blocked at PW2, the drop of liquid level that differs from the normal fluctuation of liquid level can still be obviously monitored at 60 m downstream of the blocking point. This indicates that the liquid level fluctuation caused by the blockage of the sewer can spread downstream for a long distance, indicating that a single liquid level sensor can at least complete the blockage identification of the sewer with a total of 65 m upstream and downstream. If multiple liquid level sensors are used to form a liquid level monitoring network, the monitoring range covers longer sewer, and more accurate identification and positioning of sewer blockage can be performed.

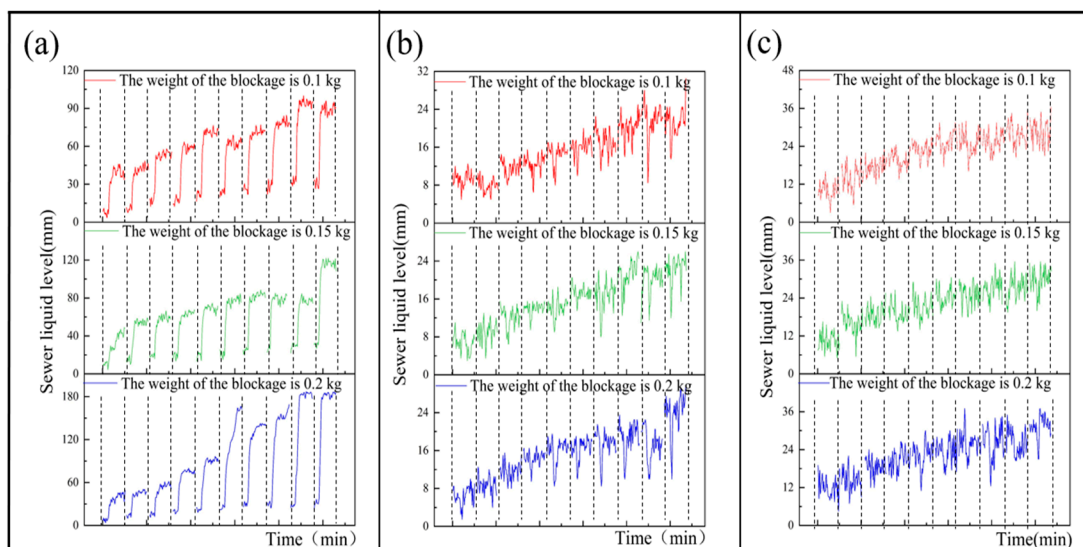


Figure 5. When the flow rate in the sewer ranges from 0.5 to 5 m³/h, the liquid level change in the upstream and downstream of the blocking point in the pipeline of DN150 at PW2: (a) The liquid level change of the DN100 sewer at PW1, and it is 1 m upstream of the blocking point; (b) The liquid level change of DN150 sewer at PW4, and it is 29.55 m downstream of the blocking point; (c) The liquid level change of DN200 sewer at PW6, and it is 60.4 m downstream of the blocking point.

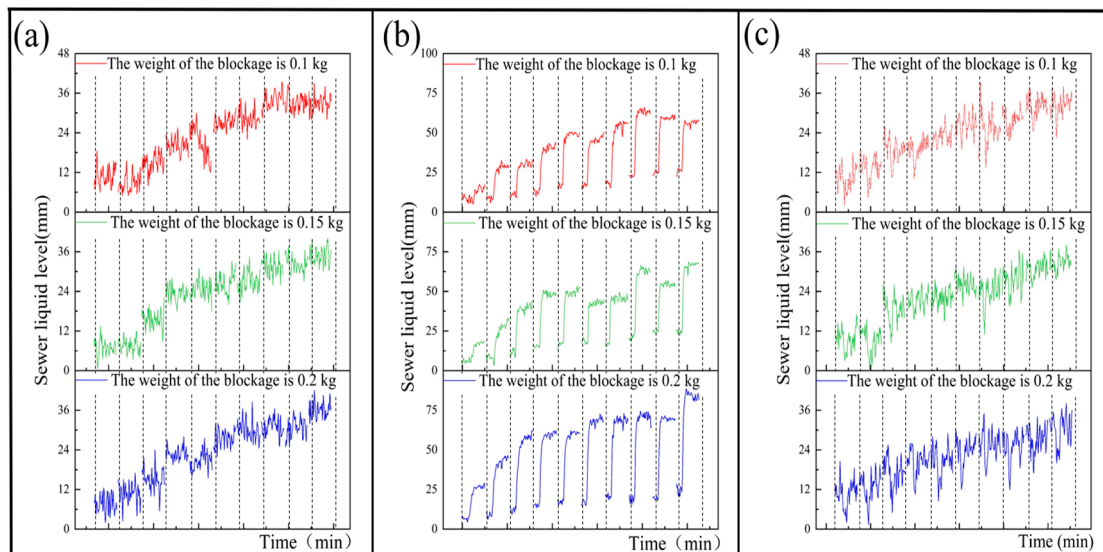


Figure 6. When the flow rate in the sewer ranges from 0.5 to $5\text{ m}^3/\text{h}$, the liquid level change in the upstream and downstream of the blocking point in the pipeline of DN200 at PW5: (a) The liquid level change of DN150 sewer at PW3, and it is 24.85 m upstream of the blocking point. (b) The liquid level change of DN200 sewer at PW4, and it is 4 m upstream of the blocking point (PW4). (c) The liquid level change of DN200 sewer at PW6, and it is 26.85 m downstream of the blocking point. The liquid level change rate and fluctuation range of the DN200 drainage pipeline under normal operating conditions and after blocking are shown in Table S1 of the annex. Annex Table S1 shows that the flow of the DN200 drainage pipe exceeds $1\text{ m}^3/\text{h}$; the minimum liquid level rise rate at 4 m upstream of the blocking point is greater than the normal liquid level fluctuation, and the liquid level rise amplitude at 4 m upstream of the blocking point exceeds 300% . For flow that is below $1\text{ m}^3/\text{h}$, the liquid level change rate upstream of the blocking point basically coincides with the range of liquid level change rate caused by normal liquid level fluctuation. When the flow rate is $0.5\text{ m}^3/\text{h}$, the liquid level at 4 m upstream of the blocking point rises from 6 mm to 17 mm , which is greater than the liquid level rise caused by normal liquid level fluctuation. In addition, this liquid level rise fluctuation is the minimum liquid level rise amplitude upstream of the blocking point after DN200 drainage pipe is blocked under this flow rate. That is, at a flow rate ranging from 0.5 to $5\text{ m}^3/\text{h}$, the blocking identification of the downstream of the level monitoring point of DN200 drainage pipeline can be completed through the two limiting conditions of the liquid level change rate and the liquid level fluctuation range. Under normal conditions, the minimum liquid level change rate of DN200 drainage pipeline is included in the range of liquid level change rate downstream of the blocking point, and the minimum liquid level drop fluctuation monitored downstream of the blocking point exceeds the maximum liquid level drop fluctuation under normal conditions. In addition, abnormal liquid level drop fluctuation can be monitored severally downstream of the blocking point. Based on this, when the flow ranges from 0.5 to $5\text{ m}^3/\text{h}$, the blocking identification of the sewer upstream of the liquid level monitoring point can be completed by the two conditions of the liquid level change rate and the liquid level change range.

According to the two blocking identification criteria of liquid level change rate and liquid level change range, the blocking condition of the DN150 and DN200 sewers were identified in the pilot-scale experiment, and the identification results are shown in Table S2 in the annex. The table shows that $0.5\text{--}5\text{ m}^3/\text{h}$ among 150 groups of monitoring data (DN150 drainage pipe was blocked, and the monitoring data at 24.85 m upstream of the blocking point were excluded), 96% of the blocking identification can be completed by the two limiting conditions of liquid level change rate and liquid level fluctuation range when the sewer was blocked to different degrees. The blocking identification rate within 4 m upstream of the blocking point was 95.3% , which was attributed to the fact that the liquid level monitoring point upstream of the blocking point was close to the blocking

point. The identification rate at the downstream of the blocking point was 93.3%, and the blockage with 0.2 kg dry weight can be 100% identified as blocking at 29.55 m and 60.4 m downstream of the blocking point. The identification rate of the drainage pipe blockage caused by 0.15 kg and 0.1 kg dry weight blockage was 93.3%. Evidently, this method positively affects the identification and positioning of sewer blockage. However, when the liquid level monitoring point was in far proximity from the blocking point, the liquid level sensor has difficulty quickly monitoring the rise in the liquid level. The liquid level monitoring point downstream of the blocking point can quickly and accurately complete blocking identification. After the level sensor detects abnormal liquid level, the relative position of the blocking point to the level sensor is determined according to the number of the level sensor and the change in the liquid level to the positioning of the blocking point.

3.2. Full-Scale Experiment Analysis of Sewer Blockage Identification

The full-scale experiment was conducted on the left sewer in Figure 3 to identify and position the blockage. The experiment was conducted in the low peak and peak water consumption periods, respectively. The data processing method of the full-scale experiment was the same as that of the pilot-scale experiment. The liquid level change was shown in Figures 7 and 8.

Figures 7 and 8 show that the full-scale experiment of sewer blockage identification and positioning was conducted in two periods of low peak and peak water consumption. Owing to the small number of local residents and dispersed population, the liquid level in both periods was low. After the DN300 sewer was blocked, the liquid level drop different from the normal liquid level fluctuation can be detected at the liquid level monitoring point downstream of the blocking point, which is marked in Figures 7 and 8. No obvious liquid level change was detected at the upstream of the blocking point, which also proved that in the pilot-scale experiment, the liquid level at the upstream of the blocking point rose, but it was difficult to monitor the obvious liquid level rise when the liquid level sensor was far away from the blocking point. For the change of liquid level downstream of the blockage point, it is not difficult to find from Figures 7 and 8 that a significant drop in liquid level can be detected at the downstream level monitoring point and marked with a red arrow. For these monitored level drops, the level change rate and level change range are summarized.

3.3. Data-Driven Models for Sewer Blockage Prediction

To meet the requirements of sewer online monitoring, the use of the liquid level sensor is indispensable, but the huge amount of data poses new challenges. Owing to the emergence of the data driven model, this online fault monitoring mode supported by a huge amount of data is more effective and accurate. Based on the discriminant analysis model of double threshold, a data-driven model for the identification and position of sewer blockage is established, and the threshold is calculated through the data processed by pilot-scale experiments and full-scale experiments.

The discriminant analysis model was used to analyze the sewer of DN200 in pilot-scale experiment and the sewer of DN300 in field-scale experiment. The normal operation and blocking of sewers are defined as 0 and 1, respectively. The dependent variables are liquid level and liquid level change rate; the level and level change rate are defined as X1 and X2, respectively, and the results of the blocking discriminant analysis model are shown in Table 3. The resulting blocking discriminant model re-predicts the initial data of the above model, and the prediction results are shown in Table 4. It can be seen from Table 4 that 19.4% of the liquid level change data of DN200 sewer in normal operation in the pilot-scale experiment will be judged to be blocked, resulting in misjudgment. In the pilot-scale experiment, after the sewer of DN200 was blocked, 20% of the blockages were misjudged as the normal operation, and the total blockage judgment success rate of 80% in the pilot experiment was acceptable. In the full-scale experiment, the sewer was not misjudged as obstruction under the normal operation of the sewer, and 83.3% of the cases after the sewer was blocked can be successfully identified as blockage; an acceptable 16.7% of the drop in

level after blockage could not be judged blocked. The overall success rates of pilot-scale experiments and full-scale experiments for the normal operation and blockage of sewers were 80.4% and 95.6%, respectively, and the discriminant model had good effects.

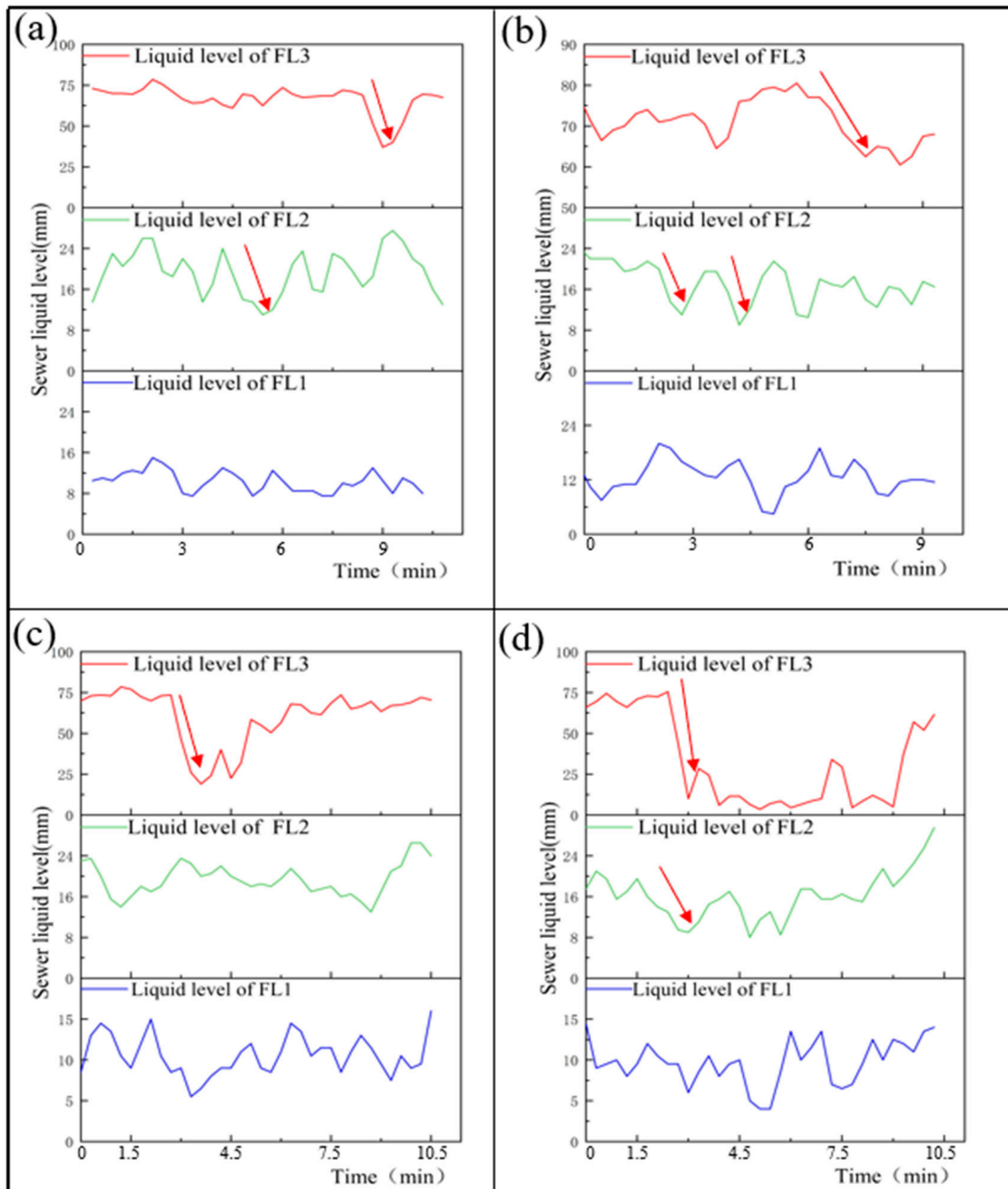


Figure 7. During the low water consumption period, the liquid level change in the upstream and downstream of the DN300 sewer blocking point. (a) The upstream and downstream liquid level change of the blocking point when the DN300 sewer was blocked at FW1. (b) The upstream and downstream liquid level change of the blocking point when the DN300 sewer was blocked at FW2. (c) The upstream and downstream liquid level change of the blocking point when the DN300 sewer was blocked at FW3. (d) The upstream and downstream liquid level change of the blocking point when the DN300 sewer was blocked at FW4. The arrows are pointing at when blockage happened.

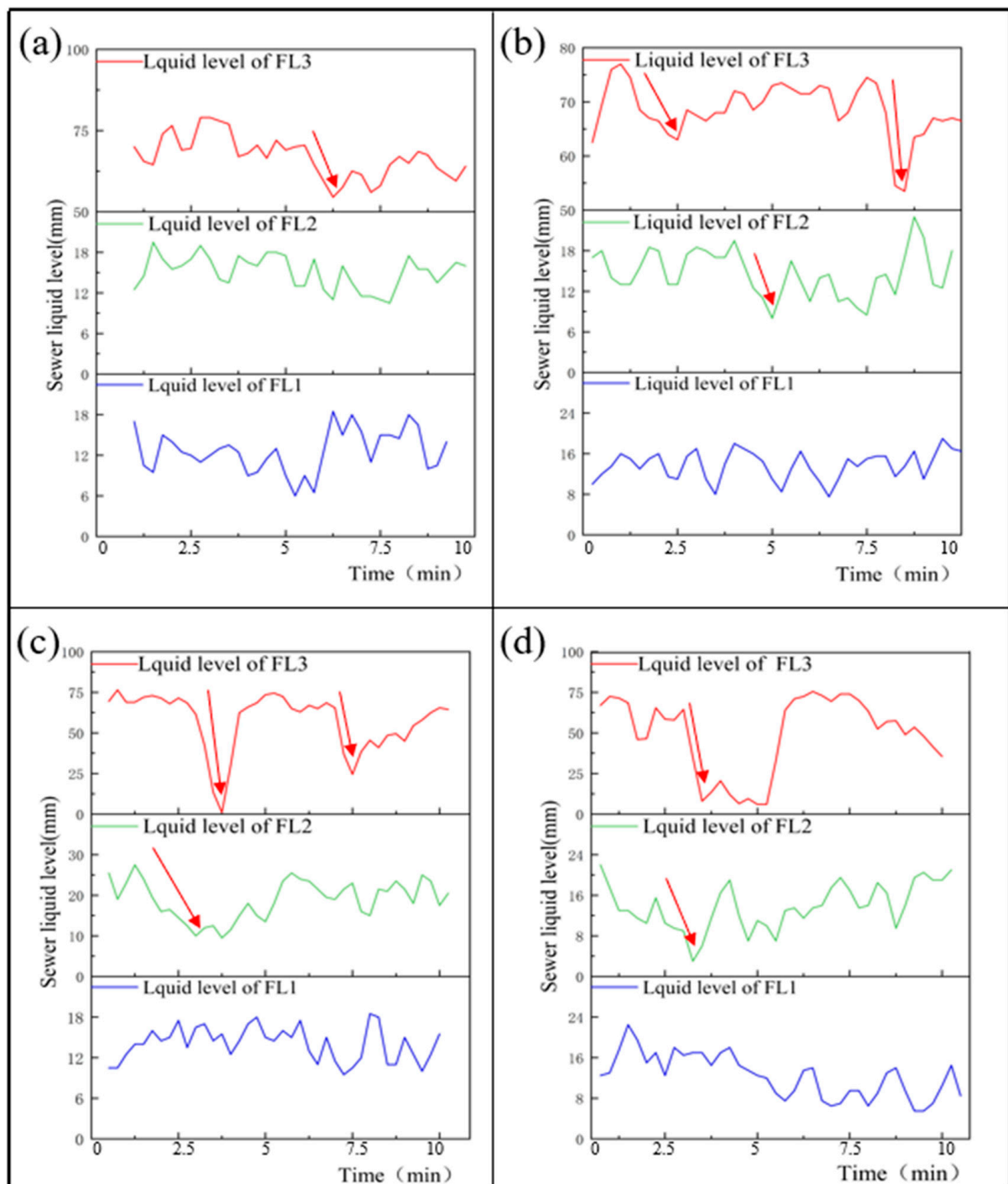


Figure 8. Change in the liquid level upstream and downstream of the DN300 sewer blocking point during the peak water consumption. (a) The upstream and downstream liquid level change of the blocking point when the DN300 sewer was blocked at FW1. (b) The upstream and downstream liquid level change of the blocking point when the DN300 sewer was blocked at FW2. (c) The upstream and downstream liquid level change of the blocking point when the DN300 sewer was blocked at FW3. (d) The upstream and downstream liquid level change of the blocking point when the DN300 sewer was blocked at FW4. The arrows are pointing at when blockage happened.

Table 3. Sewer blockage discriminant model coefficient.

Diameter	DN200		DN300	
Blockage	0	1	0	1
X_1	0.306	0.218	0.049	0.032
X_2	−0.2	−0.439	−0.039	−0.250
constant	5.637	−8.444	−1.894	−12.053

Table 4. Sewer blockage identification model prediction group results.

Prediction Group Results	DN200 Sewer Blockage			DN300 Sewer Blockage		
Blockage	0	1	Total	0	1	Total
0	25	6	31	50	0	50
1	5	20	25	3	15	18
0 (%)	80.60%	19.40%	100%	100%	0	100%
1 (%)	20.00%	80.00%	100%	16.70%	83.30%	100%
The total prediction success rate is 80.4%			The total prediction success rate is 95.60%			

3.4. Blockage Identification

The pilot-scale experiment of this study can provide the liquid level change rate and liquid level fluctuation range of DN200 sewer in normal operation and after blocking, and the full-scale experiment can provide the liquid level change rate and liquid level fluctuation range of DN300 sewer in normal operation and after blocking. Based on the induction and analysis of the above results, the identification method of sewer blockage can be represented by the matrix in Tables 5 and 6. Table 5 shows that the flow is 0.5–5 m³/h; the threshold value of the two factors, i.e., the change rate of liquid level and the fluctuation range of liquid level upstream of the blocking point of DN200 sewer, is related to the flow. When flow ranges from 0.5 to 5 m³/h, the threshold values of the two factors, i.e., the change rate of liquid level and fluctuation range of liquid level downstream of the blocking point of DN200 sewer, fluctuate within a certain range and have no obvious relationship with the flow. The lower limit range of the threshold value of the liquid level change rate and the liquid level fluctuation range at the upstream of the blocking point ranges from 14 to 56 mm/min and 11 to 39 mm, respectively, and the upper limit range of the threshold value of the liquid level change rate and the liquid level fluctuation range at the downstream of the blocking point ranges from −12 to −30 mm/min and −5.5 to −14 mm, respectively. If the liquid level of a liquid level sensor exceeds the threshold value of the liquid level change rate and liquid level fluctuation range at the same time, it can be identified as blocking and the position of the blocking point can be identified according to its liquid level change rate and liquid level change value. For the DN300 sewer, Table 6 shows that the range of normal liquid level fluctuation and liquid level change rate ranges. Furthermore, when the flow rate is less than 1 m³/h, if its liquid level drop rate is below −28 mm/min, and the liquid level drop range exceeds 10 mm, the upstream of the liquid level monitoring point is considered to be blocked. Similarly, at a flow rate of 1 m³/h to 5 m³/h, if its liquid level drop rate is below −50 mm/min, and the liquid level drop range exceeds 20 mm, the upstream of the liquid level monitoring point is considered to be blocked.

Table 5. Sewer blockage identification matrix of DN200.

Q (m ³ /h)	The Sewer of DN200 Is Blocked			
	Level Change Rate Threshold of the Blocking Point (mm/min)		Level Fluctuation Range Threshold of the Blocking Point (mm)	
	Upstream (Lower Limit)	Downstream (Upper Limit)	Upstream (Lower Limit)	Downstream (Upper Limit)
0.5	14	−16	11	−8
1	18	−16	19	−9.5
1.5	30	−16	21	−5.5
2	36	−14	28	−9.5
2.5	46	−12	33	−8
3	42	−12	27	−11
3.5	48	−30	28	−13.5
4	56	−20	39	−9.5
4.5	48	−16	31	−11
5	46	−24	32	−14

Table 6. Sewer blockage identification matrix of DN300.

Q (m ³ /h)	The Sewer of DN300 Is Blocked		The Sewer of DN300 Is Normal	
	Level Change Rate Threshold of the Downstream Blocking Point (mm/min)	Level Fluctuation Range Threshold of the Downstream Blocking Point (mm)	The Range of Liquid Level Change Rate (mm/min)	Maximum Liquid Level Fluctuation Range (mm)
0–1	−28	−10	−26–30	−7.5
1–5	−50	−20	−34–38	−14.5

For the normal operation of the sewer level change rate and liquid level change range, we are through the level sensor under the normal operating conditions of the sewer after a long time to obtain the extreme value, through the actual monitoring found that the probability of such extreme value is relatively low. In addition, under normal operating conditions, the extreme value of the liquid level change rate and the liquid level change range are calculated and summarized separately; that is, the extreme value of the liquid level change rate and the extreme value of the liquid level change range appear at different times, and we sort out these extreme values, and it is rare for the double threshold of the sewer to meet the double threshold of blocking discrimination under the normal operation of the sewer.

3.5. Discussions

In this study, the double threshold method composed of liquid level change rate and liquid level change range was used to identify the sewer blockage, and the liquid level change rate and liquid level change matrix after normal operation and blockage of sewer were obtained through pilot-scale experiments and full-scale experiments. By deploying multiple level sensors to form a monitoring network, massive level monitoring is possible. The liquid level sensor completes the real-time acquisition of liquid level data and calculates the real-time change rate and level change range of liquid level after data processing. If the level change rate is negative and small, blockage may occur, and it is necessary to select the matching flow range according to the liquid level range before the liquid level drops or in combination with the flow meter and then select the threshold. Then, the real-time monitoring of the liquid level drop rate and the liquid level change range are compared with the double threshold, and if the double threshold is met at the same time, it is judged to be blocked. According to the layout position of the level sensor, the position of the blocked pipe section relative to the level sensor can be determined, and the sewer can be identified and positioned. From full-scale experiments, it can be seen that after the sewer where the upstream manhole FW1 is blocked, the downstream FL3 can still detect a significant drop in liquid level, and it can be seen that the level sensor can detect the change of liquid level after blockage 180 m upstream of it. Although the liquid level change can

still be monitored at a long distance downstream after the upstream blockage, in order to improve the effect of blocking identification, it is advisable not to exceed 100 m. The discriminant model was used to establish the liquid level under normal conditions and after blockage based on the double threshold method. Taking the original liquid level data as the prediction group, the prediction group results showed that the success rate of sewer blockage of DN200 was 80%, and the overall success rate was 80.4%. The success rate of sewer blockage of DN300 was 83.3%, and the overall success rate was 95.6%, indicating that this method had a good effect on identifying sewer blockage.

Hassouna et al. [22] used three different data mining methods (decision trees, logical regression, and random forest) to establish a prediction model and used event duration monitors (EDM) and sewer level monitors to predict the blockage of sewer. All of Hassouna et al.'s models have an accuracy rate of more than 89% and have the potential to predict. However, the worst is undoubtedly the Logistic regression model, with an accuracy of 89.69% in the first stage and an improvement of 0.01 in the second stage. It was followed by the random forest model with an accuracy rate of 95.77%, and the decision tree was the optimal model with an accuracy rate of 95.78%. In this study, a blocking prediction model is also established based on the liquid level data of the time series. In contrast, this study uses the double threshold method to predict the blockage from the aspects of liquid level change rate and liquid level change range, mainly including the normal operation of drainage pipelines and the prediction after blockage so as to test the feasibility of online monitoring and early warning. Ugarelli et al. [26] used historical sewer blockage data in Oslo to show that sewage pipelines are more prone to blockages than combined flow and storm-water pipelines. The diameter and slope of sewers have an inverse relationship with the tendency of blockages to occur, and the likelihood of blockages increases as the age increases. Bailey et al. [27] use decision trees to study the impact of basic characteristics of sewer (length, diameter, gradient) on the risk of blockage. Ugarelli and Bailey tend to explain the influence of various factors on the blockage of sewers from a macroscopic perspective, and this study distinguishes blockage from normal from the perspective of the change law of liquid level after blockage during sewer operation so as to achieve the purpose of blockage prediction.

4. Conclusions

The fast and accurate identification and positioning of sewer blockage allows for the operation and maintenance of sewers and can reduce the amount of earthwork excavation required. Therefore, performing the identification and positioning experiment of sewer blockage is highly significant. In this study, a large number of pilot-scale experiments with a flow rate of 0.5–5 m³/h were carried out to identify the rule of liquid level change rate and liquid level change amplitude under DN200 normal operation conditions and after blocking determines the threshold value of liquid level change rate and liquid level change amplitude for blocking identification. The liquid level change rate and liquid level change threshold of DN300 drainage pipe blockage identification in different water use periods were determined using field experiments. Through full-scale experiments, the threshold of liquid level change rate and the liquid level change range for DN300 sewer blockage identification in different water use periods were determined. At the end, the article summarizes the liquid level change rate and liquid level change amplitude threshold for blockage identification with different pipe diameters. Using pilot-scale experiment and full-scale experiment data to establish a model and using the discriminant model to repredict it, the prediction accuracy rate is close to 80%, and reasonable determination of the threshold is the key to improving the accuracy of blocking recognition.

Supplementary Materials: The following supporting information can be downloaded at: <https://www.mdpi.com/article/10.3390/pr11010161/s1>, Table S1: Summary table of liquid level change rate and fluctuation range of DN200 drainage pipeline under normal operation and after blocking; Table S2: Results of blockage identification through upstream and downstream liquid level monitoring of DN150 and DN200 drainage pipes after blockage.

Author Contributions: Conceptualization, X.W.; methodology, N.L. and X.W.; formal analysis, N.L. and Z.L.; investigation, N.L.; resources, A.N. and J.Z.; writing—original draft preparation, N.L.; writing—review and editing, X.W.; project administration, X.W.; supervision, F.Z.; validation, C.L.; funding acquisition, X.W. All authors have read and agreed to the published version of the manuscript.

Funding: This work was funded by the National Key R&D Program of China (grant number 2020YFD1100303).

Data Availability Statement: Data will be made available on request.

Acknowledgments: The author would like to acknowledge the field support provided by Rongcheng Water Group Co., Ltd. and Qingdao Licunhe WWTP.

Conflicts of Interest: The authors declare no conflict of interest.

References

1. Ministry of Housing and Urban–Rural Development of China. Statistical Bulletin of Urban and Rural Construction in 2016. Available online: https://www.mohurd.gov.cn/gongkai/fdzdgnr/sjfb/tjxx/tjgb/201708/20170822_232983.html (accessed on 22 August 2017).
2. American Society of Civil Engineers. 2017 Infrastructure Report Card—Wastewater. 2017. Available online: <https://www.infrastructurereportcard.org/wp-content/uploads/2017/01/Wastewater-Final.pdf> (accessed on 6 September 2019).
3. Haurum, J.B.; Moeslund, T.B. A Survey on Image-Based Automation of CCTV and SSET Sewer Inspections. *Autom. Constr.* **2020**, *111*, 103031. [\[CrossRef\]](#)
4. Huang, D.; Liu, X.; Jiang, S.; Wang, H.; Wang, J.; Zhang, Y. Current State and Future Perspectives of Sewer Networks in Urban China. *Front. Environ. Sci. Eng.* **2018**, *12*, 1–16. [\[CrossRef\]](#)
5. Rodríguez, J.P.; McIntyre, N.; Díaz-Granados, M.; Maksimović, Č. A Database and Model to Support Proactive Management of Sediment-Related Sewer Blockages. *Water Res.* **2012**, *46*, 4571–4586. [\[CrossRef\]](#) [\[PubMed\]](#)
6. Ugarelli, R.; Kristensen, S.M.; Røstum, J.; Sægrov, S.; di Federico, V. Statistical Analysis and Definition of Block ages-Prediction Formulae for the Wastewater Network of Oslo by Evolutionary Computing. *Water Sci. Technol.* **2009**, *59*, 1457–1470. [\[CrossRef\]](#) [\[PubMed\]](#)
7. Quiñones-Grueiro, M.; Bernal-de Lázaro, J.M.; Verde, C.; Prieto-Moreno, A.; Llanes-Santiago, O. Comparison of Classifiers for Leak Location in Water Distribution Networks. *IFAC-PapersOnLine* **2018**, *51*, 407–413. [\[CrossRef\]](#)
8. Dhananchezhyan, P.; Hiremath, S.S.; Singaperumal, M.; Ramakrishnan, R. Design and Development of a Reconfigurable Type Autonomous Sewage Cleaning Mobile Manipulator. *Procedia Eng.* **2013**, *64*, 1464–1473. [\[CrossRef\]](#)
9. Li, X.; Yu, W.; Lin, X.; Iyengar, S.S. On Optimizing Autonomous Pipeline Inspection. *IEEE Trans. Robot.* **2012**, *28*, 223–233. [\[CrossRef\]](#)
10. Lu, C.P.; Huang, H.P.; Yan, J.L.; Cheng, T.H. Development of a Pipe Inspection Robot. In Proceedings of the IECON 2007-33rd Annual Conference of the IEEE Industrial Electronics Society, Taipei, Taiwan, 5–8 November 2007; pp. 626–631. [\[CrossRef\]](#)
11. Pullan, P.; Niranjan, V. Intelligent Clogged Sewer Control System. In Proceedings of the 2019 IEEE International WIE Conference on Electrical and Computer Engineering (WIECON-ECE), Bangalore, India, 15–16 November 2019; pp. 1–4. [\[CrossRef\]](#)
12. Kahi, S.E.; Asmar, D.; Fakhri, A.; Nieto, J.; Nebot, E. A vision-based system for mapping the inside of a pipe. In Proceedings of the 2011 IEEE International Conference on Robotics and Biomimetics, Karon Beach, Thailand, 7–11 December 2011; pp. 2605–2611. [\[CrossRef\]](#)
13. Nayak, A.; Pradhan, S.K. Design of a New In-Pipe Inspection Robot. *Procedia Eng.* **2014**, *97*, 2081–2091. [\[CrossRef\]](#)
14. Ajin, M.; Satheesh Kumar, G.; Karthikeyan, P. Design, Structural and Kinematic Analysis of Reconfigurable Sewage Cleaning Robot. *Appl. Mech. Mater.* **2016**, *852*, 763–769. [\[CrossRef\]](#)
15. Khan, M.S. Empirical Modeling of Acoustic Signal Attenuation in Municipal Sewer Pipes for Condition Monitoring Applications. In Proceedings of the IEEE Green Technologies Conference, IEEE Computer Society, Austin, TX, USA, 5 June 2018; pp. 137–143. [\[CrossRef\]](#)
16. Yu, Y.; Safari, A.; Niu, X.; Drinkwater, B.; Horoshenkov, K.V. Acoustic and Ultrasonic Techniques for Defect Detection and Condition Monitoring in Water and Sewerage Pipes: A Review. *Appl. Acoust.* **2021**, *183*, 108282. [\[CrossRef\]](#)
17. Adegboye, M.A.; Fung, W.K.; Karnik, A. Recent Advances in Pipeline Monitoring and Oil Leakage Detection Technologies: Principles and Approaches. *Sensors* **2019**, *19*, 2548. [\[CrossRef\]](#) [\[PubMed\]](#)

18. Villez, K. Qualitative Trend Analysis for Process Monitoring and Supervision Based on Likelihood Optimization: State-of-the-Art and Current Limitations. *IFAC Proc.* **2014**, *47*, 7140–7145. [[CrossRef](#)]
19. Thürlimann, C.M.; Dürrenmatt, D.J.; Villez, K. Soft-Sensing with Qualitative Trend Analysis for Wastewater Treatment Plant Control. *Control Eng. Pract.* **2018**, *70*, 121–133. [[CrossRef](#)]
20. Rayhana, R.; Jiao, Y.; Zaji, A.; Liu, Z. Automated Vision Systems for Condition Assessment of Sewer and Water Pipelines. *IEEE Trans. Autom. Sci. Eng.* **2021**, *18*, 1861–1878. [[CrossRef](#)]
21. Harvey, R.R.; McBean, E.A. Comparing the Utility of Decision Trees and Support Vector Machines When Planning Inspections of Linear Sewer Infrastructure. *J. Hydroinformatics.* **2014**, *16*, 1265–1279. [[CrossRef](#)]
22. Hassouna, M.; Reis, M.; Al Fairuz, M.; Tarhini, A. Data-Driven Models for Sewer Blockage Prediction. In Proceedings of the 2019 International Conference on Computing, Electronics & Communications Engineering (iCCECE), London, UK, 22–23 August 2019; pp. 68–72. [[CrossRef](#)]
23. Singh, M.; Ahmed, S. IoT Based Smart Water Management Systems: A Systematic Review. *Mater Today Proc.* **2021**, *46*, 5211–5218. [[CrossRef](#)]
24. Canali, C.; De Cicco, G.; Morten, B.; Prudenziati, M.; Taroni, A. Temperature Compensated Ultrasonic Sensor Operating in Air for Distance and Proximity Measurements. In *IEEE Transactions on Industrial Electronics*; IEEE: Greenville, SC, USA, 1982; Volume 29, pp. 336–341. [[CrossRef](#)]
25. Hansun, S. A new approach of moving average method in time series analysis. In Proceedings of the 2013 Conference on New Media Studies (CoNMedia), Tangerang, Indonesia, 27–28 November 2013; pp. 1–4. [[CrossRef](#)]
26. Ugarelli, R.; Venkatesh, G.; Brattebø, H.; Di Federico, V.; Sægrov, S. Historical analysis of blockages in wastewater pipelines in Oslo and diagnosis of causative pipeline characteristics. *Urban Water J.* **2010**, *7*, 335–343. [[CrossRef](#)]
27. Bailey, J.; Keedwell, E.; Djordjevic, S.; Kapelan, Z.; Burton, C.; Harris, E. Predictive risk modelling of real-world wastewater network incidents. *Procedia Eng.* **2015**, *119*, 1288–1298. [[CrossRef](#)]

Disclaimer/Publisher's Note: The statements, opinions and data contained in all publications are solely those of the individual author(s) and contributor(s) and not of MDPI and/or the editor(s). MDPI and/or the editor(s) disclaim responsibility for any injury to people or property resulting from any ideas, methods, instructions or products referred to in the content.